Observation of an a_0-like State with Mass of 1.817 GeV in the Study of $D_s^+ \to K_S^0 K^+ \pi^0$ Decays

M. Ablikim,[1] M. N. Achasov,[11,b] P. Adlarson,[70] M. Albrecht,[4] R. Aliberti,[30] A. Amoroso,[69a,69c] M. R. An,[34] Q. An,[65,52] X. H. Bai,[60] Y. Bai,[51] O. Bakina,[31] R. Baldini Ferroli,[25a] I. Balossino,[26a] Y. Ban,[41,g] V. Batozskaya,[1,39] D. Becker,[30] K. Begzsuren,[28] N. Berger,[30] M. Bertani,[25a] D. Bettoni,[26a] F. Bianchi,[69a,69c] J. Bloms,[63] A. Bortone,[69a,69c] I. Boyko,[31] R. A. Briere,[5] A. Brueggemann,[63] H. Cai,[71] X. Cai,[1,52] A. Calcaterra,[25a] G. F. Cao,[1,57] N. Cao,[1,57] S. A. Cetin,[56a] J. F. Chang,[1,52] W. L. Chang,[1,57] G. Chelkov,[31,a] C. Chen,[38] G. Chen,[1] H. S. Chen,[1,57] M. L. Chen,[1,52] S. J. Chen,[37] T. Chen,[1] X. R. Chen,[27,57] X. T. Chen,[1] Y. B. Chen,[1,52] Z. J. Chen,[22,h] W. S. Cheng,[69c] G. Cibinetto,[26a] F. Cossio,[69c] J. J. Cui,[44] H. L. Dai,[1,52] J. P. Dai,[73] A. Dbeyssi,[16] R. E. de Boer,[4] D. Dedovich,[31] Z. Y. Deng,[1] A. Denig,[30] I. Denysenko,[31] M. Destefanis,[69a,69c] F. De Mori,[69a,69c] Y. Ding,[35] J. Dong,[1,52] L. Y. Dong,[1,57] M. Y. Dong,[1,52,57] X. Dong,[71] S. X. Du,[75] P. Egorov,[31,a] Y. L. Fan,[71] J. Fang,[1,52] S. S. Fang,[1,57] Y. Fang,[1] R. Farinelli,[26a] L. Fava,[69b,69c] F. Feldbauer,[5] G. Felici,[25a] C. Q. Feng,[66,52] J. H. Feng,[53] K. Fischer,[64] M. Fritsch,[4] C. Fritzsch,[63] C. D. Fu,[1] H. Gao,[57] Y. N. Gao,[41,g] Yang Gao,[66,52] S. Garbolino,[69c] I. Garzia,[26a,26b] P. T. Ge,[71] Z. W. Ge,[37] C. Geng,[53] E. M. Gersabeck,[61] A. Gilman,[62] L. Gong,[35] W. X. Gong,[1,52] W. Gradl,[30] M. Greco,[69a,69c] L. M. Gu,[37] M. H. Gu,[1,52] Y. T. Gu,[14] C. Y. Guan,[1,57] A. Q. Guo,[27,57] L. B. Guo,[36] R. P. Guo,[43] Y. P. Guo,[10,f] A. Guskov,[31,a] T. T. Han,[42] W. Y. Han,[34] X. Q. Hao,[17] F. A. Harris,[59] K. K. He,[49] K. L. He,[1,57] F. H. Heinsius,[4] C. H. Heinz,[30] Y. K. Heng,[1,52,57] C. Herold,[54] T. Holtmann,[4] G. Y. Hou,[1,57] Y. R. Hou,[57] Z. L. Hou,[1] H. M. Hu,[1,57] J. F. Hu,[50,i] T. Hu,[1,52,57] Y. Hu,[1] G. S. Huang,[66,52] K. X. Huang,[53] L. Q. Huang,[67] L. Q. Huang,[27,57] X. T. Huang,[44] Y. P. Huang,[1] Z. Huang,[41,g] T. Hussain,[66] N. Hüsken,[24,30] W. Imoehl,[24] M. Irshad,[66,52] J. Jackson,[24] S. Jaeger,[4] S. Janchiv,[28] Q. Ji,[1] Q. P. Ji,[17] X. B. Ji,[1,57] X. L. Ji,[1,52] Y. Y. Ji,[44] Z. K. Jia,[66,52] H. B. Jiang,[44] S. S. Jiang,[34] X. S. Jiang,[1,52,57] Y. Jiang,[57] J. B. Jiao,[44] Z. Jiao,[20] S. Jin,[37] Y. Jin,[60] M. Q. Jing,[1,57] T. Johansson,[70] N. Kalantar-Nayestanaki,[58] X. S. Kang,[35] R. Kappert,[58] M. Kavatsyuk,[58] B. C. Ke,[75] I. K. Keshk,[4] A. Khoukaz,[63] P. Kiese,[30] R. Kiuchi,[1] L. Koch,[32] O. B. Kolcu,[56a] B. Kopf,[4] M. Kuemmel,[4] M. Kuessner,[4] A. Kupsc,[39,70] W. Kühn,[32] J. J. Lane,[61] J. S. Lange,[32] P. Larin,[16] A. Lavania,[23] L. Lavezzi,[69a,69c] Z. H. Lei,[66,52] H. Leithoff,[30] M. Lellmann,[30] T. Lenz,[30] C. Li,[38] C. Li,[42] C. H. Li,[34] Cheng Li,[66,52] D. M. Li,[75] F. Li,[1,52] G. Li,[1] H. Li,[66,52] H. Li,[38] H. B. Li,[1,57] H. J. Li,[17] H. N. Li,[50,i] J. Q. Li,[4] J. S. Li,[53] J. W. Li,[44] Ke Li,[1] L. J. Li,[1] L. K. Li,[1] Lei Li,[3] M. H. Li,[38] P. R. Li,[33,j,k] S. X. Li,[10] S. Y. Li,[55] T. Li,[44] W. D. Li,[1,57] W. G. Li,[1] X. H. Li,[66,52] X. L. Li,[44] Xiaoyu Li,[1,57] H. Liang,[66,52] H. Liang,[29] H. Liang,[1,57] Y. F. Liang,[48] Y. T. Liang,[27,57] G. R. Liao,[13] L. Z. Liao,[44] J. Libby,[23] A. Limphirat,[54] C. X. Lin,[53] D. X. Lin,[27,57] T. Lin,[1] B. J. Liu,[1] C. X. Liu,[1] D. Liu,[16,66] F. H. Liu,[47] Fang Liu,[1] Feng Liu,[6] G. M. Liu,[50,i] H. Liu,[33,j,k] H. B. Liu,[14] H. M. Liu,[1,57] Huanhuan Liu,[1] Huihui Liu,[18] J. B. Liu,[66,52] J. L. Liu,[67] J. Y. Liu,[1,57] K. Liu,[1] K. Y. Liu,[35] Ke Liu,[19] L. Liu,[66,52] M. H. Liu,[10,f] P. L. Liu,[1] Q. Liu,[57] S. B. Liu,[66,52] T. Liu,[10,f] W. K. Liu,[38] W. M. Liu,[66,52] X. Liu,[33,j,k] Y. Liu,[33,j,k] Y. B. Liu,[38] Z. A. Liu,[1,52,57] Z. Q. Liu,[44] X. C. Lou,[1,52,57] F. X. Lu,[53] H. J. Lu,[20] J. G. Lu,[1,52] X. L. Lu,[1] Y. Lu,[7] Y. P. Lu,[1,52] Z. H. Lu,[1] C. L. Luo,[36] M. X. Luo,[74] T. Luo,[10,f] X. L. Luo,[1,52] X. R. Lyu,[57] Y. F. Lyu,[38] F. C. Ma,[35] H. L. Ma,[1] L. L. Ma,[44] M. M. Ma,[1,57] Q. M. Ma,[1] R. Q. Ma,[1,57] R. T. Ma,[57] X. Y. Ma,[1,52] Y. Ma,[41,g] F. E. Maas,[16] M. Maggiora,[69a,69c] S. Maldaner,[4] S. Malde,[64] Q. A. Malik,[68] A. Mangoni,[25b] Y. J. Mao,[41,g] Z. P. Mao,[1] S. Marcello,[69a,69c] Z. X. Meng,[60] J. G. Messchendorp,[58,12] G. Mezzadri,[26a] H. Miao,[1] T. J. Min,[37] R. E. Mitchell,[24] X. H. Mo,[1,52,57] N. Yu. Muchnoi,[11,b] H. Muramatsu,[62] Y. Nefedov,[31] F. Nerling,[12,d] I. B. Nikolaev,[11,b] Z. Ning,[1,52] S. Nisar,[9,l] Y. Niu,[44] S. L. Olsen,[57] Q. Ouyang,[1,52,57] S. Pacetti,[25b,25c] X. Pan,[10,f] Y. Pan,[61] A. Pathak,[1] A. Pathak,[29] M. Pelizaeus,[4] H. P. Peng,[66,52] J. Pettersson,[70] J. L. Ping,[36] R. G. Ping,[1,57] S. Plura,[30] S. Pogodin,[31] R. Poling,[62] V. Prasad,[66,52] H. Qi,[66,52] H. R. Qi,[55] M. Qi,[37] T. Y. Qi,[10,f] S. Qian,[1,52] W. B. Qian,[57] Z. Qian,[53] C. F. Qiao,[57] J. J. Qin,[67] L. Q. Qin,[13] X. P. Qin,[10,f] X. S. Qin,[44] Z. H. Qin,[1,52] J. F. Qiu,[1] S. Q. Qu,[55] S. Q. Qu,[38] K. H. Rashid,[68] C. F. Redmer,[30] K. J. Ren,[34] A. Rivetti,[69c] V. Rodin,[58] M. Rolo,[69c] G. Rong,[1,57] Ch. Rosner,[16] S. N. Ruan,[38] H. S. Sang,[66] A. Sarantsev,[31,c] Y. Schelhaas,[30] C. Schnier,[4] K. Schoenning,[70] M. Scodeggio,[26a,26b] K. Y. Shan,[10,f] W. Shan,[21] X. Y. Shan,[66,52] J. F. Shangguan,[49] L. G. Shao,[1,57] M. Shao,[66,52] C. P. Shen,[10,f] H. F. Shen,[1,57] X. Y. Shen,[1,57] B.-A. Shi,[57] H. C. Shi,[66,52] R. S. Shi,[1,57] X. Shi,[1,52] X. D. Shi,[66,52] J. J. Song,[17] W. M. Song,[29,1] Y. X. Song,[41,g] S. Sosio,[69a,69c] S. Spataro,[69a,69c] F. Stieler,[30] K. X. Su,[71] P. P. Su,[49] Y.-J. Su,[57] G. X. Sun,[1] H. Sun,[57] H. K. Sun,[1] J. F. Sun,[17] L. Sun,[71] S. S. Sun,[1,57] T. Sun,[1,57] W. Y. Sun,[29] X. Sun,[22,h] Y. J. Sun,[66,52] Y. Z. Sun,[1] Z. T. Sun,[42] Y. H. Tan,[71] Y. X. Tan,[66,52] C. J. Tang,[48] G. Y. Tang,[1] J. Tang,[53] L. Y. Tao,[67] Q. T. Tao,[22,h] J. X. Teng,[66,52] V. Thoren,[70] W. H. Tian,[46] Y. Tian,[27,57] I. Uman,[56b] B. Wang,[1] B. L. Wang,[57] C. W. Wang,[37] D. Y. Wang,[41,g] F. Wang,[67] H. J. Wang,[33,j,k] H. P. Wang,[1,57] K. Wang,[1,52] L. L. Wang,[1] M. Wang,[44] M. Z. Wang,[41,g] Meng Wang,[1,57] S. Wang,[10,f] T. Wang,[10,f] T. J. Wang,[38] W. Wang,[53] W. H. Wang,[71]

W. P. Wang,[66,52] X. Wang,[41,g] X. F. Wang,[33,j,k] X. L. Wang,[10,f] Y. D. Wang,[40] Y. F. Wang,[1,52,57] Y. H. Wang,[42] Y. Q. Wang,[1,57] Z. Wang,[1,52] Z. Y. Wang,[1,57] Ziyi Wang,[57] D. H. Wei,[13] F. Weidner,[63] S. P. Wen,[1] D. J. White,[61] U. Wiedner,[4] G. Wilkinson,[64] M. Wolke,[70] L. Wollenberg,[4] J. F. Wu,[1,57] L. H. Wu,[1] L. J. Wu,[1,57] X. Wu,[9,f] X. H. Wu,[29] Y. Wu,[66] Z. Wu,[1,52] L. Xia,[66,52] T. Xiang,[42,g] D. Xiao,[33,j,k] G. Y. Xiao,[37] H. Xiao,[10,f] S. Y. Xiao,[1] Y. L. Xiao,[10,f] Z. J. Xiao,[36] C. Xie,[37] X. H. Xie,[41,g] Y. Xie,[44] Y. G. Xie,[1,52] Y. H. Xie,[6] Z. P. Xie,[66,52] T. Y. Xing,[1,57] C. F. Xu,[1] C. J. Xu,[53] G. F. Xu,[1] H. Y. Xu,[60] Q. J. Xu,[15] S. Y. Xu,[65] X. P. Xu,[49] Y. C. Xu,[57] Z. P. Xu,[37] F. Yan,[10,f] L. Yan,[10,f] W. B. Yan,[66,52] W. C. Yan,[75] H. J. Yang,[45,e] H. L. Yang,[29] H. X. Yang,[1] L. Yang,[46] S. L. Yang,[57] Y. X. Yang,[1,57] Yifan Yang,[1,57] M. Ye,[1,57] M. H. Ye,[8] J. H. Yin,[1] Z. Y. You,[53] B. X. Yu,[1,52,57] C. X. Yu,[38] G. Yu,[1,57] T. Yu,[67] C. Z. Yuan,[1,57] L. Yuan,[2] S. C. Yuan,[1] X. Q. Yuan,[1] Y. Yuan,[1,57] Z. Y. Yuan,[53] C. X. Yue,[34] A. A. Zafar,[68] F. R. Zeng,[44] X. Zeng,[6] Y. Zeng,[22,h] Y. H. Zhan,[53] A. Q. Zhang,[1] B. L. Zhang,[1] B. X. Zhang,[1] G. Y. Zhang,[17] H. Zhang,[66] H. H. Zhang,[53] H. H. Zhang,[29] H. Y. Zhang,[1,52] J. L. Zhang,[72] J. Q. Zhang,[36] J. W. Zhang,[1,52,57] J. X. Zhang,[33,j,k] J. Y. Zhang,[1] J. Z. Zhang,[1,57] Jianyu Zhang,[1,57] Jiawei Zhang,[1,57] L. M. Zhang,[55] L. Q. Zhang,[53] Lei Zhang,[37] P. Zhang,[1] Q. Y. Zhang,[34,75] Shulei Zhang,[22,h] X. D. Zhang,[40] X. M. Zhang,[1] X. Y. Zhang,[44] X. Y. Zhang,[49] Y. Zhang,[64] Y. T. Zhang,[75] Y. H. Zhang,[1,52] Yan Zhang,[66,52] Yao Zhang,[1] Z. H. Zhang,[1] Z. Y. Zhang,[38] Z. Y. Zhang,[71] G. Zhao,[1] J. Zhao,[34] J. Y. Zhao,[1,57] J. Z. Zhao,[1,52] Lei Zhao,[66,52] Ling Zhao,[1] M. G. Zhao,[38] Q. Zhao,[1] S. J. Zhao,[75] Y. B. Zhao,[1,52] Y. X. Zhao,[27,58] Z. G. Zhao,[66,52] A. Zhemchugov,[31,a] B. Zheng,[67] J. P. Zheng,[1,52] Y. H. Zheng,[57] B. Zhong,[36] C. Zhong,[67] X. Zhong,[53] H. Zhou,[44] L. P. Zhou,[1,57] X. Zhou,[71] X. K. Zhou,[57] X. R. Zhou,[66,52] X. Y. Zhou,[34] Y. Z. Zhou,[10,f] J. Zhu,[38] K. Zhu,[1] K. J. Zhu,[1,52,57] L. X. Zhu,[57] S. H. Zhu,[65] S. Q. Zhu,[37] T. J. Zhu,[72] W. J. Zhu,[10,f] Y. C. Zhu,[66,52] Z. A. Zhu,[1,57] B. S. Zou,[1] and J. H. Zou[1]

(BESIII Collaboration)

[1]*Institute of High Energy Physics, Beijing 100049, People's Republic of China*
[2]*Beihang University, Beijing 100191, People's Republic of China*
[3]*Beijing Institute of Petrochemical Technology, Beijing 102617, People's Republic of China*
[4]*Bochum Ruhr-University, D-44780 Bochum, Germany*
[5]*Carnegie Mellon University, Pittsburgh, Pennsylvania 15213, USA*
[6]*Central China Normal University, Wuhan 430079, People's Republic of China*
[7]*Central South University, Changsha 410083, People's Republic of China*
[8]*China Center of Advanced Science and Technology, Beijing 100190, People's Republic of China*
[9]*COMSATS University Islamabad, Lahore Campus, Defence Road, Off Raiwind Road, 54000 Lahore, Pakistan*
[10]*Fudan University, Shanghai 200433, People's Republic of China*
[11]*G.I. Budker Institute of Nuclear Physics SB RAS (BINP), Novosibirsk 630090, Russia*
[12]*GSI Helmholtzcentre for Heavy Ion Research GmbH, D-64291 Darmstadt, Germany*
[13]*Guangxi Normal University, Guilin 541004, People's Republic of China*
[14]*Guangxi University, Nanning 530004, People's Republic of China*
[15]*Hangzhou Normal University, Hangzhou 310036, People's Republic of China*
[16]*Helmholtz Institute Mainz, Staudinger Weg 18, D-55099 Mainz, Germany*
[17]*Henan Normal University, Xinxiang 453007, People's Republic of China*
[18]*Henan University of Science and Technology, Luoyang 471003, People's Republic of China*
[19]*Henan University of Technology, Zhengzhou 450001, People's Republic of China*
[20]*Huangshan College, Huangshan 245000, People's Republic of China*
[21]*Hunan Normal University, Changsha 410081, People's Republic of China*
[22]*Hunan University, Changsha 410082, People's Republic of China*
[23]*Indian Institute of Technology Madras, Chennai 600036, India*
[24]*Indiana University, Bloomington, Indiana 47405, USA*
[25a]*INFN Laboratori Nazionali di Frascati, INFN Laboratori Nazionali di Frascati, I-00044 Frascati, Italy*
[25b]*INFN Sezione di Perugia, I-06100 Perugia, Italy*
[25c]*INFN Sezione di Perugia, I-06100 Perugia, Italy*
[25d]*University of Perugia, I-06100 Perugia, Italy*
[26a]*INFN Sezione di Ferrara, INFN Sezione di Ferrara, I-44122 Ferrara, Italy*
[26b]*University of Ferrara, I-44122 Ferrara, Italy*
[27]*Institute of Modern Physics, Lanzhou 730000, People's Republic of China*
[28]*Institute of Physics and Technology, Peace Ave. 54B, Ulaanbaatar 13330, Mongolia*
[29]*Jilin University, Changchun 130012, People's Republic of China*
[30]*Johannes Gutenberg University of Mainz, Johann-Joachim-Becher-Weg 45, D-55099 Mainz, Germany*
[31]*Joint Institute for Nuclear Research, 141980 Dubna, Moscow region, Russia*
[32]*Justus-Liebig-Universitaet Giessen, II. Physikalisches Institut, Heinrich-Buff-Ring 16, D-35392 Giessen, Germany*

[33]Lanzhou University, Lanzhou 730000, People's Republic of China
[34]Liaoning Normal University, Dalian 116029, People's Republic of China
[35]Liaoning University, Shenyang 110036, People's Republic of China
[36]Nanjing Normal University, Nanjing 210023, People's Republic of China
[37]Nanjing University, Nanjing 210093, People's Republic of China
[38]Nankai University, Tianjin 300071, People's Republic of China
[39]National Centre for Nuclear Research, Warsaw 02-093, Poland
[40]North China Electric Power University, Beijing 102206, People's Republic of China
[41]Peking University, Beijing 100871, People's Republic of China
[42]Qufu Normal University, Qufu 273165, People's Republic of China
[43]Shandong Normal University, Jinan 250014, People's Republic of China
[44]Shandong University, Jinan 250100, People's Republic of China
[45]Shanghai Jiao Tong University, Shanghai 200240, People's Republic of China
[46]Shanxi Normal University, Linfen 041004, People's Republic of China
[47]Shanxi University, Taiyuan 030006, People's Republic of China
[48]Sichuan University, Chengdu 610064, People's Republic of China
[49]Soochow University, Suzhou 215006, People's Republic of China
[50]South China Normal University, Guangzhou 510006, People's Republic of China
[51]Southeast University, Nanjing 211100, People's Republic of China
[52]State Key Laboratory of Particle Detection and Electronics, Beijing 100049, Hefei 230026, People's Republic of China
[53]Sun Yat-Sen University, Guangzhou 510275, People's Republic of China
[54]Suranaree University of Technology, University Avenue 111, Nakhon Ratchasima 30000, Thailand
[55]Tsinghua University, Beijing 100084, People's Republic of China
[56a]Turkish Accelerator Center Particle Factory Group, Istinye University, 34010, Istanbul, Turkey
[56b]Near East University, Nicosia, North Cyprus, Mersin 10, Turkey
[57]University of Chinese Academy of Sciences, Beijing 100049, People's Republic of China
[58]University of Groningen, NL-9747 AA Groningen, Netherlands
[59]University of Hawaii, Honolulu, Hawaii 96822, USA
[60]University of Jinan, Jinan 250022, People's Republic of China
[61]University of Manchester, Oxford Road, Manchester M13 9PL, United Kingdom
[62]University of Minnesota, Minneapolis, Minnesota 55455, USA
[63]University of Muenster, Wilhelm-Klemm-Str. 9, 48149 Muenster, Germany
[64]University of Oxford, Keble Rd, Oxford, United Kingdom OX13RH
[65]University of Science and Technology Liaoning, Anshan 114051, People's Republic of China
[66]University of Science and Technology of China, Hefei 230026, People's Republic of China
[67]University of South China, Hengyang 421001, People's Republic of China
[68]University of the Punjab, Lahore-54590, Pakistan
[69a]University of Turin and INFN, University of Turin, I-10125 Turin, Italy
[69b]University of Eastern Piedmont, I-15121 Alessandria, Italy
[69c]INFN, I-10125 Turin, Italy
[70]Uppsala University, Box 516, SE-75120 Uppsala, Sweden
[71]Wuhan University, Wuhan 430072, People's Republic of China
[72]Xinyang Normal University, Xinyang 464000, People's Republic of China
[73]Yunnan University, Kunming 650500, People's Republic of China
[74]Zhejiang University, Hangzhou 310027, People's Republic of China
[75]Zhengzhou University, Zhengzhou 450001, People's Republic of China

(Received 24 April 2022; revised 8 July 2022; accepted 13 September 2022; published 28 October 2022)

Using e^+e^- annihilation data corresponding to an integrated luminosity of 6.32 fb^{-1} collected at center-of-mass energies between 4.178 and 4.226 GeV with the BESIII detector, we perform the first amplitude analysis of the decay $D_s^+ \to K_S^0 K^+ \pi^0$ and determine the relative branching fractions and phases for intermediate processes. We observe an a_0-like state with mass of 1.817 GeV in its decay to $K_S^0 K^+$ for the first time. In addition, we measure the ratio $\{\mathcal{B}[D_s^+ \to \bar{K}^*(892)^0 K^+]/\mathcal{B}[D_s^+ \to \bar{K}^0 K^*(892)^+]\}$ to be

$2.35^{+0.42}_{-0.23\text{stat}} \pm 0.10_{\text{syst}}$. Finally, we provide a precision measurement of the absolute branching fraction $\mathcal{B}(D_s^+ \to K_S^0 K^+ \pi^0) = (1.46 \pm 0.06_{\text{stat}} \pm 0.05_{\text{syst}})\%$.

DOI: 10.1103/PhysRevLett.129.182001

The constituent quark model describes mesons as bound $q\bar{q}$ states grouped into SU(3) flavor multiplets. In this scenario, the $f_0(500)$ and $f_0(980)$ are often classified as the ground states of the scalar mesons with isospin-zero and the $a_0(980)$ meson is taken as their isospin-one partner. The $f_0(1370)$, $f_0(1500)$, and $a_0(1450)$ are then considered to be the corresponding radially excited states. Within the next higher set of excitations, however, which includes the $f_0(1710)$ and $f_0(1770)$, the meson with isospin-one [i.e., the $a_0(1710)$] has been proposed but has not yet been well established [1–6]. The $f_0(1710)$ is often considered to be a likely candidate for a glueball or $K^*\bar{K}^*$ molecule. Although the recent measurement of the branching fraction (BF) ratio $\mathcal{B}[f_0(1710) \to \eta\eta']/\mathcal{B}[f_0(1710) \to \pi\pi]$ [7,8] supports the hypothesis that the $f_0(1710)$ has a large glueball component, one decisive way to determine whether the $f_0(1710)$ is a glueball or $K^*\bar{K}^*$ molecule is to search for and investigate its isospin-one partner.

The *BABAR* experiment reported a new resonance [called $a_0(1700)$ in its paper] with a mass of $1704 \pm 5_{\text{stat}} \pm 2_{\text{syst}}$ MeV/c^2 and a width of $110 \pm 15_{\text{stat}} \pm 11_{\text{syst}}$ MeV on the $\pi^\pm\eta$ mass spectrum of the process $\eta_c \to \pi^+\pi^-\eta$ [9]. In addition, the BESIII experiment reported interference between the $f_0(1710)$ and a neutral a_0^0 state in amplitude analyses of $D_s^+ \to K_S^0 K_S^0 \pi^+$ and $D_s^+ \to K^+K^-\pi^+$ [10,11]. These facts inspire some exciting questions, such as whether these two new observed a_0's are in a set of isospin triplet or two irrelevant resonances, and whether a new $a_0^+ \to K_S^0 K^+$ decay can be found to establish the whole picture. Reference [2] predicts the product BF of $D_s^+ \to a_0(1710)^+\pi^0$ with $a_0(1710)^+ \to K_S^0 K^+$ to be $(1.3 \pm 0.4) \times 10^{-3}$, and Refs. [5,6] also expect that the $K_S^0 K^+$ invariant mass distribution of this process will reveal the $a_0(1710)^+$ signal. However, Ref. [12] claims that the new a_0^0 observed in the D_s^+ decays is more suitable as the isospin-one partner of the $X(1812)$ and forms a Regge trajectory along with $a_0(980)$ and $a_0(1450)$, which suggests the possibility of allotting them into a family of scalar mesons with isospin-one. Therefore, an amplitude analysis of $D_s^+ \to K_S^0 K^+ \pi^0$ provides an ideal opportunity to study the new $a_0^+ \to K_S^0 K^+$ decay and is crucial to pin down the nature of the new a_0(s) [called $a_0(1817)$ in this Letter].

The internal quark structure of the light scalar mesons, like the $a_0(980)$, have also been the source of much theoretical speculation. They have been considered to be $q\bar{q}$, $qq\bar{q}\,\bar{q}$, $K\bar{K}$, etc. The coupling constants, $g_{a_0\pi\eta}$ and g_{a_0KK}, are predicted by various models [13–15] and therefore serve as important experimental constraints on theoretical models. Combining an analysis of $D_s^+ \to K_S^0 K^+ \pi^0$ with a previous measurement of $D_s^+ \to \pi^+\pi^0\eta$ [16], we can determine the ratio $\{\mathcal{B}[a_0(980) \to K\bar{K}]/\mathcal{B}[a_0(980) \to \eta\pi]\}$. This is a key experimental input for the calculation of the coupling constants of the $a_0(980)$ and helps determine its quark composition [13–15,17–21].

Furthermore, Ref. [22] predicts that $\mathcal{B}[D_s^+ \to \bar{K}^*(892)^0 K^+]$ is greater than $\mathcal{B}[D_s^+ \to \bar{K}^0 K^*(892)^+]$, but the current experimental uncertainties are too large to verify this [23]. In an analysis of $D_s^+ \to K_S^0 K^+ \pi^0$, we can measure the BFs of both modes simultaneously. Thus, the correlated systematic uncertainties arising from the masses and widths of the resonances, the model parameters, and the common backgrounds can be considered and reduced.

Because of its large BF, the Cabibbo-favored $D_s^+ \to K_S^0 K^+ \pi^0$ decay is one of the golden decay channels of the D_s^+. This decay can be used as a reference channel for other decays of the D_s^+ meson and it is important for our understanding of B_s^0 decays to final states involving the D_s^+ mesons [23]. The CLEO experiment measured the absolute BF of the $D_s^+ \to K_S^0 K^+ \pi^0$ decay to be $(1.52 \pm 0.09_{\text{stat}} \pm 0.20_{\text{syst}})\%$ [24], using 586 pb^{-1} of e^+e^- collisions recorded at a center-of-mass energy of 4.17 GeV.

In this Letter, we present the first amplitude analysis and a more precise measurement of the BF for the decay $D_s^+ \to K_S^0 K^+ \pi^0$ using 6.32 fb^{-1} of data collected with the BESIII detector at center-of-mass energies between 4.178 and 4.226 GeV. Charge-conjugated modes are implied throughout this Letter.

The BESIII detector [25,26] records symmetric e^+e^- collisions provided by the BEPCII storage ring [27]. The cylindrical core of the BESIII detector covers 93% of the full solid angle and consists of a helium-based multilayer drift chamber (MDC), a plastic scintillator time-of-flight system (TOF), and a CsI(Tl) electromagnetic calorimeter (EMC), which are all enclosed in a superconducting solenoidal magnet providing a 1.0 T magnetic field. The end cap TOF system was upgraded in 2015 using multigap resistive plate chamber technology [28].

Simulated data samples produced with a GEANT4-based [29] Monte Carlo (MC) package, which includes the geometric description of the BESIII detector and the detector response, are used to determine detection efficiencies and to estimate backgrounds. The beam energy spread and initial state radiation (ISR) in the e^+e^- annihilations are simulated with the generator KKMC [30]. The inclusive MC sample includes the production of open charm

processes, the ISR production of vector charmonium(-like) states, and the continuum processes incorporated in KKMC [30]. The known decay modes are described with EVTGEN [31] using BFs taken from the Particle Data Group [23], and the remaining unknown charmonium decays are generated with LUNDCHARM [32]. Final state radiation (FSR) from charged final state particles is incorporated using PHOTOS [33].

We reconstruct the process $e^+e^- \to D_s^{*+}D_s^- \to \gamma D_s^+ D_s^-$ using both single-tag (ST) and double-tag (DT) candidate events [34]. An ST candidate is an event where only the D_s^- meson is reconstructed through particular hadronic decays (tag modes) without any requirement on the remaining measured tracks and EMC showers. A DT candidate is an event where the D_s^+ is reconstructed through $D_s^+ \to K_S^0 K^+ \pi^0$ in addition to the D_s^- being reconstructed through the tag modes. Eight tag modes are used: $D_s^- \to K_S^0 K^-$, $K^+K^-\pi^-$, $K^+K^-\pi^-\pi^0$, $K_S^0K^-\pi^-\pi^+$, $K_S^0K^+\pi^-\pi^-$, $\pi^-\pi^-\pi^+$, $\pi^-\eta'$, and $K^-\pi^-\pi^+$. The selection criteria for the final state particles, transition photon, and the $D_s^\pm$ candidates are the same as Refs. [35–37]. The K_S^0, π^0, η, and η' mesons are reconstructed through $K_S^0 \to \pi^+\pi^-$, $\pi^0 \to \gamma\gamma$, $\eta \to \gamma\gamma$, and $\eta' \to \pi^+\pi^-\eta$ decays, respectively.

An eight-constraint kinematic fit is applied to the DT candidates to select signal events for the amplitude analysis. The total four-momentum is constrained to the four-momentum of the e^+e^- system, and the invariant masses of the K_S^0, π^0, D_s^-, and $D_s^{*+(-)}$ candidates are constrained to their corresponding known masses [23]. Within each event, the candidate with the minimum χ^2 from the kinematic fit is chosen. The invariant mass of the signal D_s^+ is then required to be within $(1.930, 1.990)$ GeV/c^2. A ninth constraint, on the mass of the signal D_s^+, is then added to the kinematic fit to guarantee all candidates lie inside the allowed phase space. There are 1050 DT events obtained for the amplitude analysis with a signal purity of $(94.7 \pm 0.7)\%$, which is determined from a fit to the invariant mass distribution of the signal D_s^+ candidates.

The intermediate resonance composition is determined using a unbinned maximum-likelihood fit. The likelihood function is described by a signal probability density function (PDF), $|\mathcal{M}(p_j)|^2$, incoherently added to a background PDF, denoted as B [36–38]. The signal amplitude $\mathcal{M}$ is constructed based on the isobar model formulation [39]. The background PDF is constructed from inclusive MC samples using RooNDKeysPdf [40]. RooNDKeysPdf is a kernel estimation method [41] implemented in RooFit [40], which models the distribution of an input dataset as a superposition of Gaussian kernels. The likelihood function is then written as

$$\mathcal{L} = \prod_k \left[\frac{\epsilon f_s |\mathcal{M}(p_k^\mu)|^2 R_3}{\int \epsilon |\mathcal{M}(p_k^\mu)|^2 R_3 dp_k} + \frac{(1-f_s)B(p_k^\mu)R_3}{\int \epsilon B(p_k^\mu) R_3 dp_k} \right], \quad (1)$$

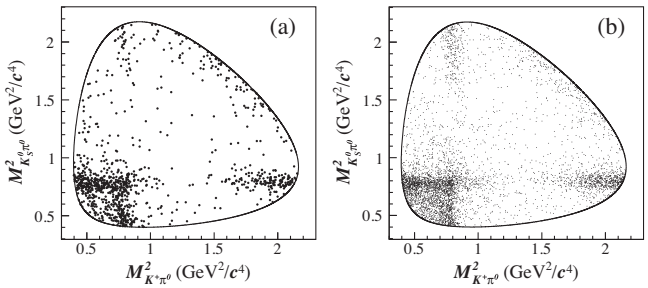

FIG. 1. The Dalitz plot of $M^2_{K_S^0\pi^0}$ versus $M^2_{K^+\pi^0}$ for the decay $D_s^+ \to K_S^0 K^+ \pi^0$ from (a) the data sample and (b) the inclusive MC sample generated based on the results of the amplitude analysis. The black curve indicates the kinematic boundary.

where ϵ is the acceptance function, the index k runs over selected events, p_k^μ represents the four-momenta of the final particles in the kth event, f_s is the signal purity, and R_3 is an element of three-body phase space. The normalization integral in the denominator is calculated by MC integration [36].

The signal amplitude $\mathcal{M}$ is a coherent sum of the amplitudes for the intermediate processes, $\mathcal{M} = \sum c_n \mathcal{A}_n$, where n indicates the nth intermediate state. The complex coefficient c_n equals $\rho_n e^{i\phi_n}$ with magnitude ρ_n and phase ϕ_n. The amplitude $\mathcal{A}_n$ is the product of the spin factor [39], the Blatt-Weisskopf barriers of the intermediate state and the D_s^+ meson [42], and the relativistic Breit-Wigner function [43] to describe the propagator for the intermediate resonance. Note that a Flatté formula [44] coupled to $K\bar{K}$ and $K^*\bar{K}^*$ for the $a_0(1817)^+$ propagator should be a better model. However, the relativistic Breit-Wigner function is still used due to the limited experimental statistics and lack of knowledge about coupling constants [45].

The $M^2_{K_S^0\pi^0}$ versus $M^2_{K^+\pi^0}$ Dalitz plot, shown in Fig. 1, reveals there is a strong contribution from the process $D_s^+ \to \bar{K}^*(892)^0 K^+$, which appears as the horizontal band around 0.8 GeV^2/c^4. Besides this dominant intermediate process, other possible intermediate resonances are considered, including the $K_0^*(700)$, $K^*(892)$, $K^*(1410)$, $K_0^*(1430)$, $K_2^*(1430)$, $K^*(1680)$, $a_0(980)$, $a_2(1320)$, $a_0(1450)$, $a_2(1700)$, $a_0(1817)$, $\rho(1700)$, and the $(K\pi)_{\mathrm{S\,wave}}$ (using the LASS parametrization [46] and the K matrix [47]). Each possibility is added to the fit one at a time. Various combinations of these resonances are tested as well. The statistical significance of each amplitude is calculated based on the change of the log-likelihood with and without this amplitude after taking the change of the degrees of freedom into account. If the significance of a newly added amplitude is greater than 5σ, this amplitude is kept, otherwise it is dropped. During the fit, f_s is fixed and the magnitudes and phases of all intermediate processes are floating and are measured with respect to those of the $D_s^+ \to \bar{K}^*(892)^0 K^+$. The mass and width of the $a_0(1817)^+$ are free, those of the $a_0(980)^+$ are fixed to the values given in

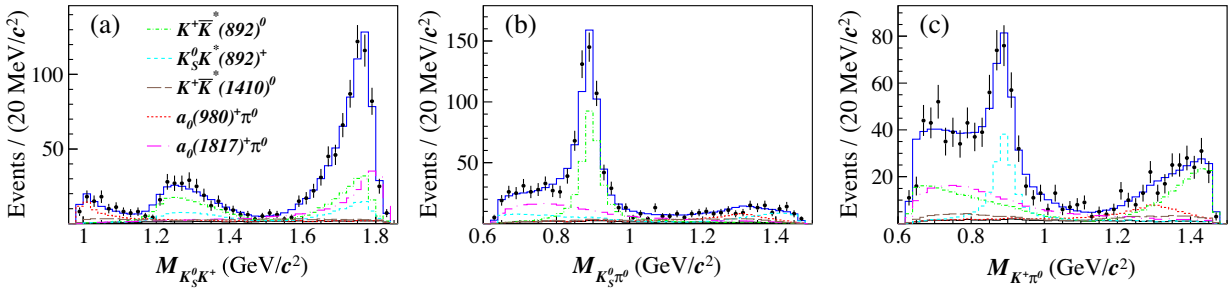

FIG. 2. The projections of the Dalitz plot onto (a) $M_{K_S^0K^+}$, (b) $M_{K_S^0\pi^0}$, and (c) $M_{K^+\pi^0}$. The data samples are represented by points with error bars, the fit results by blue lines, and backgrounds by black lines. Colored dashed lines show the components of the fit model. Because of interference effects, the fit results are not necessarily equal to the sum of the components.

Ref. [48], and those of all other resonances are fixed to their known values [23].

Five intermediate processes, $D_s^+ \to \bar{K}^*(892)^0K^+$, $D_s^+ \to K^*(892)^+K_S^0$, $D_s^+ \to a_0(980)^+\pi^0$, $D_s^+ \to \bar{K}^*(1410)^0K^+$, and $D_s^+ \to a_0(1817)^+\pi^0$, are eventually retained as the optimal set. The mass projections of the fit result are shown in Fig. 2. The contribution of the nth intermediate process relative to the total BF is quantified by a fit fraction (FF) defined as $\mathrm{FF}_n = \int|\rho_n\mathcal{A}_n|^2R_3dp_j/\int|\mathcal{M}|^2R_3dp_j$. The ratio $\{\mathcal{B}[D_s^+ \to \bar{K}^*(892)^0K^+]/\mathcal{B}[D_s^+ \to \bar{K}^0K^*(892)^+]\} = 2.35^{+0.42}_{-0.23\mathrm{stat}} \pm 0.10_{\mathrm{syst}}$ is calculated as the quotient of their FFs, where correlations are accounted for in the systematic and statistical uncertainties. The phases and FFs for the intermediate processes are listed in Table I. The mass and width of the $a_0(1817)^+$ are $(1.817 \pm 0.008_{\mathrm{stat}} \pm 0.020_{\mathrm{syst}})$ GeV/c^2 and $(0.097 \pm 0.022_{\mathrm{stat}} \pm 0.015_{\mathrm{syst}})$ GeV/c^2, respectively.

Some tests are made to further clarify the existence of the $a_0(1817)^+$. First, the recoil of the $K_0^*(700)$ may cause an enhancement at the high end of the $K_S^0K^+$ spectrum, but the shape of the $K_0^*(700)$ does not match the distribution of data and has a significance less than 3σ. Second, the log-likelihood value of a fit with the $K_0^*(700)$ included and the $a_0(1817)^+$ excluded decreases by 40 compared to the nominal fit. In addition, even though the $\rho(1700)^+$ and the $a_2(1700)^+$ peak at the same position as the $a_0(1817)^+$ in the $K_S^0K^+$ spectrum, the log-likelihood value is worse by 70 units when these resonances are included instead of the $a_0(1817)^+$.

The differences between the results of the nominal fit and the following alternative fits are assigned as the systematic uncertainties for the amplitude analysis. To estimate the systematic uncertainty related to resonances, the masses and widths of the $\bar{K}^*(892)^0$, $K^*(892)^+$, $a_0(980)^+$, and $\bar{K}^*(1410)^0$ are varied by their uncertainties [23]. The uncertainty associated with Blatt-Weisskopf barriers are studied by varying the radii by ± 1 GeV^{-1}. The uncertainty caused by background is studied by increasing or decreasing f_s within its statistical uncertainty, and by varying the proportion of MC background components according to the uncertainties of their cross section measurement. The intermediate resonances with statistical significances less than 5σ are included in the fit one by one and the largest difference with respect to the baseline fit is taken as the systematic uncertainty. The acceptance of the detector is examined by repeating the amplitude analysis fit with different particle-identification and tracking efficiencies according to their uncertainties. The total uncertainties are determined by adding all the contributions in quadrature.

To measure the absolute BF of the process $D_s^+ \to K_S^0K^+\pi^0$, we use the same event selection criteria as those for the amplitude analysis, except that the momentum of the final state π^+ originating from the signal D_s^+ meson is required to be greater than 0.1 GeV/c to remove soft pions from D^{*+} decays, and the best candidate strategy is changed. The best ST candidate from the tagged D_s^- is chosen using the recoiling mass closest to the known

TABLE I. Phases, FFs, BFs, and statistical significances (σ) of intermediate processes with the final state $K_S^0K^+\pi^0$. The first and second uncertainties are statistical and systematic, respectively. Because of interference effects, the total of the FFs is not necessarily equal to 100%.

Amplitude	Phase (rad)	FF (%)	BF (10^{-3})	σ
$D_s^+ \to \bar{K}^*(892)^0K^+$	0.0 (fixed)	$32.7 \pm 2.2 \pm 1.9$	$4.77 \pm 0.38 \pm 0.32$	> 10
$D_s^+ \to K^*(892)^+K_S^0$	$-0.16 \pm 0.12 \pm 0.11$	$13.9 \pm 1.7 \pm 1.3$	$2.03 \pm 0.26 \pm 0.20$	> 10
$D_s^+ \to a_0(980)^+\pi^0$	$-0.97 \pm 0.27 \pm 0.25$	$7.7 \pm 1.7 \pm 1.8$	$1.12 \pm 0.25 \pm 0.27$	6.7
$D_s^+ \to \bar{K}^*(1410)^0K^+$	$0.17 \pm 0.15 \pm 0.08$	$6.0 \pm 1.4 \pm 1.3$	$0.88 \pm 0.21 \pm 0.19$	7.6
$D_s^+ \to a_0(1817)^+\pi^0$	$-2.55 \pm 0.21 \pm 0.07$	$23.6 \pm 3.4 \pm 2.0$	$3.44 \pm 0.52 \pm 0.32$	> 10

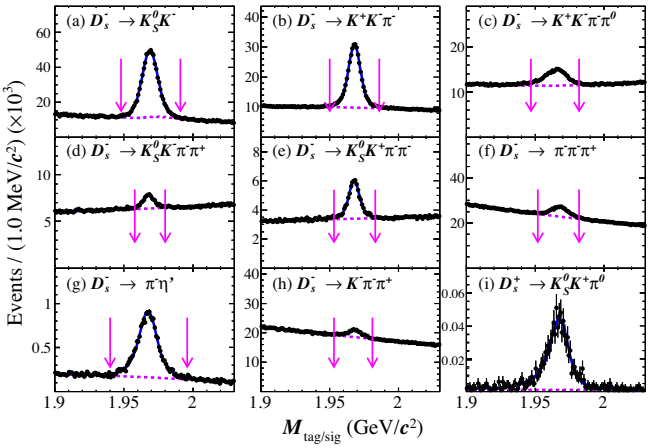

FIG. 3. Fits to (a)–(h) the $M_{\rm tag}$ distributions of the ST candidates of various tag modes and (i) the $M_{\rm sig}$ distribution of the DT candidates. The data samples are represented by points with error bars, the total fit results by blue solid lines, and backgrounds by violet dashed lines. The pairs of pink arrows indicate the signal regions.

D_s^{*+} mass [23] per tag mode. The best DT candidate is chosen using the average mass of the tagged D_s^- ($M_{\rm tag}$) and the signal D_s^+ ($M_{\rm sig}$) closest to the known D_s mass per tag mode. The BF of the $D_s^+ \to K_S^0 K^+\pi^0$ decay is determined by

$$\mathcal{B}(D_s^+ \to K_S^0 K^+\pi^0) = \frac{N_{\rm sig}^{\rm DT}}{\sum_\alpha N_\alpha^{\rm ST}\epsilon_{\alpha,{\rm sig}}^{\rm DT}/\epsilon_\alpha^{\rm ST}}, \qquad (2)$$

where α represents various tag modes. The ST yield for tag mode α, $N_\alpha^{\rm ST}$, is obtained from fits to the $M_{\rm tag}$ distributions of the ST candidates from the data sample, as shown in Figs. 3(a)–3(h). The MC-simulated shape convolved with a Gaussian function is used to model the signal shape while the background shape is parametrized by a second-order Chebyshev function. The MC-simulated shapes of $D^- \to K_S^0\pi^-$ and $D_s^- \to \eta\pi^+\pi^-\pi^-$ decays are added to the Chebyshev functions in the fits to $D_s^- \to K_S^0 K^-$ and $D_s^- \to \pi^-\eta'$, respectively, to account for peaking background. The DT yield, $N_{\rm sig}^{\rm DT}$, is determined from the fit to the $M_{\rm sig}$ distribution of the DT candidates from the data sample, as shown in Fig. 3(i), in which the signal shape is the MC-simulated shape convolved with a Gaussian function and the background shape is described by the MC-simulated background shape. The inclusive MC samples with $D_s^+ \to K_S^0 K^+\pi^0$ events generated based on the amplitude analysis are studied to determine the ST efficiencies $\epsilon_\alpha^{\rm ST}$ and DT efficiencies $\epsilon_{\alpha,{\rm sig}}^{\rm DT}$. The total ST yield of all tag modes and the DT yield are 531217 ± 2235 and 985 ± 40, respectively. The BF of the $D_s^+ \to K_S^0 K^+\pi^0$ decay is determined to be $(1.46 \pm 0.06_{\rm stat} \pm 0.05_{\rm syst})\%$. The BFs for various intermediate processes are calculated with $\mathcal{B}_i = {\rm FF}_i \times \mathcal{B}(D_s^+ \to K_S^0 K^+\pi^0)$ and the results are listed in Table I.

The systematic uncertainties on the BF measurement from the following sources are studied. The uncertainty in the total number of the ST D_s^- mesons is assigned to be 0.4%, including the changes of the fit yields when varying the signal shape, background shape, and taking into account the background fluctuation in the fit. The uncertainty associated with the background shape in the fit to the $M_{\rm sig}$ distribution is estimated to be 1.9% by replacing the nominal background shape with a second-order Chebyshev function. The uncertainty for the K_S^0 reconstruction efficiency is estimated to be 1.5% by using control samples of $J/\psi \to K_S^0 K^+\pi^-$ and $\phi K_S^0 K^+\pi^-$ decays. The K^+ particle-identification and tracking efficiencies are studied with $e^+e^- \to K^+K^-\pi^+\pi^-$ events. The data-MC differences of the K^+ particle-identification and tracking efficiencies are assigned as systematic uncertainties, which are both 1.0%. The systematic uncertainty of the π^0 reconstruction efficiency is investigated by using a control sample of the process $e^+e^- \to K^+K^-\pi^+\pi^-\pi^0$ and a 2.0% systematic uncertainty is assigned. The systematic uncertainty caused by the amplitude analysis model is studied by varying the parameters in the amplitude analysis fit according to the covariance matrix. The change of signal efficiency, 0.7%, is set as the corresponding systematic uncertainty.

In summary, this Letter presents the first amplitude analysis of the decay $D_s^+ \to K_S^0 K^+\pi^0$ using 6.32 fb^{-1} of e^+e^- annihilation data taken at center-of-mass energies between 4.178 and 4.226 GeV. The BF of $D_s^+ \to K_S^0 K^+\pi^0$ is determined to be $(1.46 \pm 0.06_{\rm stat} \pm 0.05_{\rm syst})\%$, which is consistent with the CLEO result [24]. The precision is improved by a factor of 2.8.

The phases and the FFs of intermediate states are listed in Table I. The statistical significance of $D_s^+ \to a_0(1817)^+\pi^0$ is found to be greater than 10σ. The mass and width of the $a_0(1817)^+$ are measured to be $(1.817 \pm 0.008_{\rm stat} \pm 0.020_{\rm syst})$ GeV/c^2 and $(0.097 \pm 0.022_{\rm stat} \pm 0.015_{\rm syst})$ GeV/c^2, respectively. Along with the observed enhancement at the $K_S^0 K_S^0$ mass threshold in $D_s^+ \to K_S^0 K_S^0\pi^+$ [10], our result supports the existence of a new a_0 triplet. The BF of $D_s^+ \to a_0(1817)^+\pi^0$ with $a_0(1817)^+ \to K_S^0 K^+$ is roughly consistent with the prediction [2] assuming the $a_0(1817)^+$ meson is the candidate isospin-one partner of the $f_0(1710)$ meson, proposed by Refs. [1–6]. However, the mass is about 100 MeV/c^2 greater than the predicted value. This higher mass may imply instead that this a_0-like state is the isospin-one partner of the $X(1812)$ [12]. A more sophisticated study of this a_0-like state is expected in a simultaneous amplitude analysis of $D_s^+ \to K_S^0 K^+\pi^0$ and $K_S^0 K_S^0\pi^+$ in the future.

In addition, the ratio $\{\mathcal{B}[D_s^+ \to \bar{K}^*(892)^0 K^+]/\mathcal{B}[D_s^+ \to \bar{K}^0 K^*(892)^+]\}$ is determined to be $2.35^{+0.42}_{-0.23{\rm stat}} \pm 0.10_{\rm syst}$.

The contribution of $D_s^+ \to a_0(980)^+\pi^0$ is also observed. Using $\mathcal{B}[D_s^+ \to a_0(980)^+\pi^0]$ [16], we determine the ratio $\{\mathcal{B}[a_0(980)^+ \to \bar{K}^0K^+]/\mathcal{B}[a_0(980)^+ \to \pi^+\eta]\} = (13.7 \pm 3.6_{\rm stat} \pm 4.2_{\rm syst})\%$.

The BESIII Collaboration thanks the staff of BEPCII and the IHEP computing center for their strong support. This work is supported in part by National Key R&D Program of China under Contracts No. 2020YFA0406400 and No. 2020YFA0406300; National Natural Science Foundation of China (NSFC) under Contracts No. 11625523, No. 11635010, No. 11735014, No. 11822506, No. 11835012, No. 11875054, No. 11935015, No. 11935016, No. 11935018, No. 11961141012, No. 12022510, No. 12025502, No. 12035009, No. 12035013, No. 12061131003, No. 12192260, No. 12192261, No. 12192262, No. 12192263, No. 12192264, and No. 12192265; the Chinese Academy of Sciences (CAS) Large-Scale Scientific Facility Program; Joint Large-Scale Scientific Facility Funds of the NSFC and CAS under Contracts No. U2032104, No. U1732263, and No. U1832207; CAS Key Research Program of Frontier Sciences under Contract No. QYZDJ-SSW-SLH040; 100 Talents Program of CAS; INPAC and Shanghai Key Laboratory for Particle Physics and Cosmology; ERC under Contract No. 758462; European Union Horizon 2020 research and innovation programme under Contract No. Marie Sklodowska-Curie Grant Agreement No. 894790; German Research Foundation DFG under Contracts No. 443159800, Collaborative Research Center CRC 1044, FOR 2359, FOR 2359, GRK 214; Istituto Nazionale di Fisica Nucleare, Italy; Ministry of Development of Turkey under Contract No. DPT2006K-120470; National Science and Technology fund; Olle Engkvist Foundation under Contract No. 200-0605; STFC (United Kingdom); The Knut and Alice Wallenberg Foundation (Sweden) under Contract No. 2016.0157; The Royal Society, UK under Contracts No. DH140054 and No. DH160214; The Swedish Research Council; U.S. Department of Energy under Contracts No. DE-FG02-05ER41374 and No. DE-SC-0012069.

[a]Also at the Moscow Institute of Physics and Technology, Moscow 141700, Russia.
[b]Also at the Novosibirsk State University, Novosibirsk, 630090, Russia.
[c]Also at the NRC "Kurchatov Institute", PNPI, 188300, Gatchina, Russia.
[d]Also at Goethe University Frankfurt, 60323 Frankfurt am Main, Germany.
[e]Also at Key Laboratory for Particle Physics, Astrophysics and Cosmology, Ministry of Education; Shanghai Key Laboratory for Particle Physics and Cosmology; Institute of Nuclear and Particle Physics, Shanghai 200240, People's Republic of China.
[f]Also at Key Laboratory of Nuclear Physics and Ion-beam Application (MOE) and Institute of Modern Physics, Fudan University, Shanghai 200443, People's Republic of China.
[g]Also at State Key Laboratory of Nuclear Physics and Technology, Peking University, Beijing 100871, People's Republic of China.
[h]Also at School of Physics and Electronics, Hunan University, Changsha 410082, China.
[i]Also at Guangdong Provincial Key Laboratory of Nuclear Science, Institute of Quantum Matter, South China Normal University, Guangzhou 510006, China.
[j]Also at Frontiers Science Center for Rare Isotopes, Lanzhou University, Lanzhou 730000, People's Republic of China.
[k]Also at Lanzhou Center for Theoretical Physics, Lanzhou University, Lanzhou 730000, People's Republic of China.
[l]Also at the Department of Mathematical Sciences, IBA, Karachi, Pakistan.

[1] L. S. Geng and E. Oset, Phys. Rev. D **79**, 074009 (2009).
[2] L. R. Dai, E. Oset, and L. S. Geng, Eur. Phys. J. C **82**, 225 (2022).
[3] E. Klempt, Phys. Lett. B **820**, 136512 (2021).
[4] A. V. Sarantsev, I. Denisenko, U. Thoma, and E. Klempt, Phys. Lett. B **816**, 136227 (2021).
[5] Z. L. Wang and B. S. Zou, Eur. Phys. J. C **82**, 509 (2022).
[6] X. Zhu, D. M. Li, E. Wang, L. S. Geng, and J. J. Xie, Phys. Rev. D **105**, 116010 (2022).
[7] M. Ablikim *et al.* (BESIII Collaboration), arXiv:2202.00621.
[8] M. Ablikim *et al.* (BESIII Collaboration), arXiv:2202.00623.
[9] J. P. Lees *et al.* (*BABAR* Collaboration), Phys. Rev. D **104**, 072002 (2021).
[10] M. Ablikim *et al.* (BESIII Collaboration), Phys. Rev. D **105**, L051103 (2022).
[11] M. Ablikim *et al.* (BESIII Collaboration), Phys. Rev. D **104**, 012016 (2021).
[12] D. Guo, W. Chen, H. X. Chen, X. Liu, and S. L. Zhu, Phys. Rev. D **105**, 114014 (2022).
[13] N. N. Achasov and V. N. Ivanchenko, Nucl. Phys. **B315**, 465 (1989).
[14] N. N. Achasov and V. V. Gubin, Phys. Rev. D **56**, 4084 (1997).
[15] W. Wang, Phys. Lett. B **759**, 501 (2016).
[16] M. Ablikim *et al.* (BESIII Collaboration), Phys. Rev. Lett. **123**, 112001 (2019).
[17] W. Wang and C. D. Lu, Phys. Rev. D **82**, 034016 (2010).
[18] Y. K. Hsiao, Y. Yu, and B. C. Ke, Eur. Phys. J. C **80**, 895 (2020).
[19] Y. Yu, Y. K. Hsiao, and B. C. Ke, Eur. Phys. J. C **81**, 1093 (2021).
[20] J. Y. Wang, M. Y. Duan, G. Y. Wang, D. M. Li, L. J. Liu, and E. Wang, Phys. Lett. B **821**, 136617 (2021).
[21] M. Y. Duan, J. Y. Wang, G. Y. Wang, E. Wang, and D. M. Li, Eur. Phys. J. C **80**, 1041 (2020).
[22] H. Y. Cheng and C. W. Chiang, Phys. Rev. D **100**, 093002 (2019).
[23] P. A. Zyla *et al.* (Particle Data Group), Prog. Theor. Exp. Phys. **2020**, 083C01 (2020) and 2021 update.
[24] P. U. E. Onyisi *et al.* (CLEO Collaboration), Phys. Rev. D **88**, 032009 (2013).

[25] M. Ablikim *et al.* (BESIII Collaboration), Nucl. Instrum. Methods Phys. Res., Sect. A **614**, 345 (2010).
[26] M. Ablikim *et al.* (BESIII Collaboration), Chin. Phys. C **44**, 040001 (2020).
[27] C. H. Yu *et al.*, *Proceedings of IPAC2016, Busan, Korea* (JACoW, Geneva, Switzerland, 2016), 10.18429/JACoW-IPAC2016-TUYA01.
[28] X. Li *et al.*, Radiat. Detect. Technol. Methods **1**, 13 (2017); Y. X. Guo *et al.*, Radiat. Detect. Technol. Methods **1**, 15 (2017).
[29] S. Agostinelli *et al.* (GEANT4 Collaboration), Nucl. Instrum. Methods Phys. Res., Sect. A **506**, 250 (2003).
[30] S. Jadach, B. F. L. Ward, and Z. Was, Phys. Rev. D **63**, 113009 (2001); Comput. Phys. Commun. **130**, 260 (2000).
[31] D. J. Lange, Nucl. Instrum. Methods Phys. Res., Sect. A **462**, 152 (2001); R. G. Ping, Chin. Phys. C **32**, 599 (2008).
[32] J. C. Chen, G. S. Huang, X. R. Qi, D. H. Zhang, and Y. S. Zhu, Phys. Rev. D **62**, 034003 (2000); R. L. Yang, R. G. Ping, and H. Chen, Chin. Phys. Lett. **31**, 061301 (2014).
[33] E. Richter-Was, Phys. Lett. B **303**, 163 (1993).
[34] J. Adler *et al.* (MARK-III Collaboration), Phys. Rev. Lett. **62**, 1821 (1989).
[35] M. Ablikim *et al.* (BESIII Collaboration), Phys. Rev. D **103**, 092004 (2021).
[36] M. Ablikim *et al.* (BESIII Collaboration), J. High Energy Phys. 06 (2021) 181.
[37] M. Ablikim *et al.* (BESIII Collaboration), Phys. Rev. D **103**, 092006 (2021).
[38] M. Artuso *et al.* (CLEO Collaboration), Phys. Rev. D **85**, 122002 (2012).
[39] B. S. Zou and D. V. Bugg, Eur. Phys. J. A **16**, 537 (2003).
[40] W. Verkerke and D. P. Kirkby, RooFit Users Manual v2.91 (2019).
[41] K. Cranmer, Comput. Phys. Commun. **136**, 198 (2001).
[42] J. M. Blatt and V. F. Weisskopf, *Theoretical Nuclear Physics* (John Wiley & Sons, New York, 1973).
[43] J. D. Jackson, Nuovo Cimento **34**, 1644 (1964).
[44] Z, L, Wang, and B. S. Zou, Eur. Phys. J. C **82**, 509 (2022).
[45] S. Flatté, Phys. Lett. **63B**, 224 (1976).
[46] I. Adachi *et al.* (*BABAR* and BELLE Collaboration), Phys. Rev. D **98**, 112012 (2018).
[47] A. V. Anisovich and A. V. Sarantsev, Phys. Lett. B **413**, 137 (1997).
[48] M. Albrecht *et al.* (Crystal Barrel Collaboration), Eur. Phys. J. C **80**, 453 (2020).